Menthyl-substituted Organophosphorus Compounds. Part 6.[1] Preparation of P(L-men)RCl and P(L-men)R(S)Cl (R = Me, Et, Pr^i, Bu^t, or Ph; men = *cyclo*-C_6H_9-2-Pr^i-5-Me) and Nuclear Magnetic Resonance Studies of Configuration and Halogen Exchange‡

Gerhard Hägele,* Wolfgang Kückelhaus, Gudrun Tossing, and Jürgen Seega
Institut für Anorganische Chemie und Strukturchemie I der Universität Düsseldorf, Universitätsstrasse 1, D-4000 Düsseldorf 1, Federal Republic of Germany
Robin K. Harris,*† Clifford J. Creswell, and Per T. Jageland
School of Chemical Sciences, University of East Anglia, University Plain, Norwich NR4 7TJ

Menthyl-substituted chlorophosphines P(L-men)RCl and thiophosphoryl chlorides P(L-men)R(S)Cl (R = Me, Et, or Pr^i; men = menthyl, *i.e.* 2-isopropyl-5-methylcyclohexyl) have been prepared. These series (including compounds with R = Ph and Bu^t) were subjected to ^{1}H, ^{13}C, and ^{31}P n.m.r. studies at ambient temperature. Chemical shifts of C-4, C-8, H-8, CH_3-7, CH_3-9, and CH_3-10 and the coupling constants $^2J_{PC-2}$, $^2J_{PC-4}$, $^3J_{PC-1}$, and $^3J_{PC-8}$ are stereospecific indicators for the configurations of phosphorus in P-epimeric forms of P(L-men)R(S)Cl. The values of $^2J_{PC-2}$ and $^2J_{PC-4}$ reflect effects from intramolecular rotation around the P–C(menthyl) bond. Influences from substituents R on chemical shifts and coupling constants are discussed. Variable-temperature ^{31}P n.m.r. studies using line broadening and selective inversion-recovery techniques on chlorophosphines P(L-men)PhCl and P(L-men)EtCl revealed halogen-exchange processes which are likely to have cationic phosphorus intermediates.

Interest in stereochemical and catalytic research has given rise to synthetic studies of organophosphorus compounds bearing chiral substituents. Particular attention was drawn towards menthyl (2-isopropyl-5-methylcyclohexyl, men) and neomenthyl derivatives, which are accessible by two main routes. Metallated phosphines react with menthyl- and neomenthyl-halogenides under epimerisation of C-3 to yield the corresponding neomenthyl- and menthyl-phosphorus derivatives.[2] A more convenient path to menthyl-phosphorus compounds[3] uses the classical low-temperature selective substitution of phosphorus–halogen compounds by Grignard reagents, which proceeds with retention of the menthyl skeleton.

In P(L-men)Cl_2 (**1**)[4] a single menthyl group is connected to a prochiral phosphorus atom. The two menthyl groups in P(L-men)$_2$Cl (**2a**)[5] bind to a pseudoprochiral phosphorus centre. For P(L-men)(D-men)Cl (**2b**)[1b] a pseudochiral phosphorus gives rise to two pseudo-P-epimeric forms having $R_{(P)}$ or $S_{(P)}$ configurations with a pair of enantiotopic menthyl groups each.

Since our interests concentrated towards P-chiral menthyl–phosphorus compounds we studied the synthesis of phenyl- and alkyl-substituted chloro(menthyl)phosphines P(L-men)RCl. The phenyl, methyl, and ethyl derivatives of this series are accessible by low-temperature substitution of highly reactive dichlorophosphines with L-menthylmagnesium chloride, equation (1).

$$PRCl_2 + Mg(L\text{-men})Cl \longrightarrow \underset{\substack{(2c)\ R = Ph^{1c}\\(2d)\ R = Me\\(2e)\ R = Et}}{P(L\text{-men})RCl} \qquad (1)$$

The more sterically hindered isopropyl and t-butyl compounds were obtained using the reversed reaction sequence, equation (2). For alkylchloro(L-menthyl)phosphines two P-epimeric forms having either the $R_{(P)}$ or the $S_{(P)}$ configuration are expected. For the phenyl-, ethyl-, and isopropyl-substituted compounds (**2c**), (**2e**), and (**2f**), two specific P-epimers were discovered by means of ^{31}P-{^{1}H} n.m.r. spectroscopy.

$$\underset{(1)}{P(L\text{-men})Cl_2} + MgRCl \longrightarrow \underset{\substack{(2f)\ R = Pr^i\\(2g)\ R = Bu^t}}{P(L\text{-men})RCl}{}^{1e} \qquad (2)$$

The methyl and t-butyl compounds (**2d**) and (**2g**) showed single resonance peaks, thus indicating an unlikely diastereospecific synthesis or a more likely rapid exchange reaction leading to dynamic n.m.r. systems. Detailed results of the variable-temperature n.m.r. studies on P(L-men)RCl are given later.

Menthyl-substituted chlorophosphines (**1**) and (**2a**)—(**2g**) combine with elemental sulphur to yield the corresponding thiophosphoryl chlorides, equations (3) and (4). The sterically

$$\underset{(1)}{P(L\text{-men})Cl_2} \xrightarrow{\frac{1}{8}S_8} \underset{(3)}{P(L\text{-men})(S)Cl_2} \qquad (3)$$

$$\underset{(2a)—(2g)}{P(L\text{-men})RCl} \xrightarrow{\frac{1}{8}S_8} \underset{(4a)—(4g)}{P(L\text{-men})R(S)Cl} \qquad (4)$$

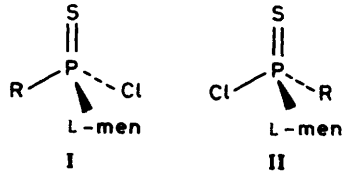

(**4c**)	R = Ph	$S_{(P)}$	$R_{(P)}$
(**4d**)	R = Me	$R_{(P)}$	$S_{(P)}$
(**4e**)	R = Et	$R_{(P)}$	$S_{(P)}$
(**4f**)	R = Pr^i	$R_{(P)}$	$S_{(P)}$
(**4g**)	R = Bu^t	$S_{(P)}$	$R_{(P)}$

Scheme 1. The P-epimeric forms I and II for P(L-men)R(S)Cl (**4c**)—(**4g**)

† *Present address:* Department of Chemistry, University of Durham, South Road, Durham DH1 3LE.

‡ *Non-S.I. unit employed:* Torr ≈ 133 N m^{-2}.

crowded thiophosphoryl chlorides (3) and (4a)—(4g) are stable towards oxygen and do not hydrolyse in the open air. The P-chiral compounds may be described by two P-epimeric forms, as shown in Scheme 1.

The sulphurisation of chlorophosphines (2c)—(2g) yielded mixtures of both P-epimeric thiophosphoryl chlorides (4c)—(4g), which are characterised by specific ^{1}H-, ^{13}C-, and ^{31}P-n.m.r. data (see below). While the ethyl and isopropyl compounds (2e) and (2f) resulted as viscous materials, we succeeded in isolating the $S_{(P)}$ form of the phenyl-substituted compound (4c) and the $R_{(P)}$ t-butyl derivative (4g). *X*-Ray studies revealed the absolute configuration of these samples [1d,e] and MNDO calculations on (4g)[6] yielded additional evidence for the molecular structure of this compound. On this basis absolute configurations were assigned to the total series P(L-men)R(S)Cl (4) as given in Scheme 1.

Results

The first striking result concerned the uniform tendency for the chemical shift values δ_P. All P-epimeric forms **I** have higher δ_P data than corresponding forms **II**. As an inconvenient result from the sequence rule of Prelog and co-workers,[7] the formal description of molecular structures having analogous geometries in form **I** assigns $R_{(P)}$ configuration to the methyl, ethyl, and isopropyl compounds, while the phenyl and t-butyl derivatives are described as $S_{(P)}$.

The situation is more complex for trivalent chlorophosphines P(L-men)RCl (2), as may be derived by comparison of the phenyl compound (2c) and the ethyl analogue (2e). The dominating form of (2c) is the high-frequency P-epimer (2c-I) with δ_P = 104.1 p.p.m. (79%), while the minor component (2c-II) has δ_P = 99.4 p.pm. (21%). Addition of sulphur to the genuine mixture (2c-I)–(2c-II) produced the P-epimeric pair of P(L-men)Ph(S)Cl (4c) with significant values for (4c-I), δ_P = 101.7 p.p.m. (76%), and (4c-II), δ_P = 97.7 p.p.m. (24%). Since sulphurisation proceeds *via* retention and since (4c-I) has the $S_{(P)}$ configuration,[1d] (2c-I) must be attributed to the $S_{(P)}$ form.

The reverse relationship holds for the ethyl compounds, however. The dominating component of P(L-men)EtCl (2e) is the low-frequency P-epimer (2e-II) with δ_P = 119.9 p.p.m.

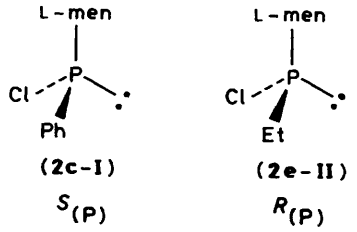

Scheme 2. The most stable P-epimers for (2c) and (2e)

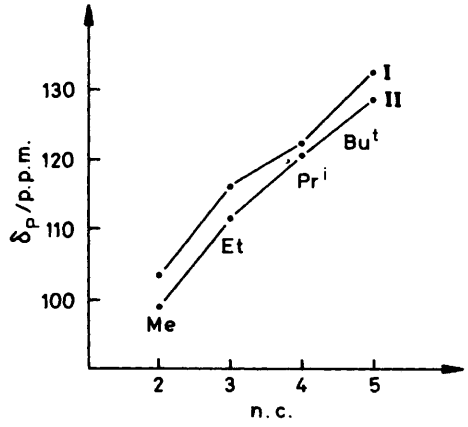

Figure 1. Substituent effects on chemical shifts δ_P of P-epimeric forms of (4d)—(4g); n.c. = number of β-carbon atoms

Table 1. Preparative results and δ_P values for L-menthyl-substituted chlorophosphines, P(L-men)RCl (2), and thiophosphoryl chlorides, P(L-men)R(S)Cl (4)

Compound	R	Yield (%)	B.p./pressure (°C/Torr)	δ_P(I)/ p.p.m.	% (I)[a]	δ_P(II)/ p.p.m.	% (II)[a]	Solution
(2c)[b]	Ph	71	135/0.5	104.1	79	99.4	21	5% in toluene[c]
				103.4	72	98.5	28	5% in thf[c]
				103.85	n.c.	98.82	n.c.	30% in $C_6D_5CD_3$[d]
(2d)	Me	56	78—80/0.2	108.9	r.e.	108.9	r.e.	pure[c]
				107.4	r.e.	107.4	r.e.	5% in thf[c]
				109.19	r.e.	109.19	r.e.	70% in C_6D_6[d]
(2e)	Et	64	95/0.2	122.5	29	119.9	71	pure[c]
				123.1	31	120.8	69	5% in thf[c]
				123.25	n.c.	123.24	n.c.	70% in C_6D_6[d]
(2f)	Pr^i	45	112/0.4	124.7	30	121.4	70	5% in thf[c]
				123.25	r.e.	123.25	r.e.	70% in C_6D_6[d]
(2g)[e]	Bu^t	77	118/0.9	132.2	r.e.	132.2	r.e.	pure[c]
				131.8	r.e.	131.8	r.e.	5% in toluene[d]
(4c)[b,f]	Ph	71		101.7	76/34	97.7	24/66	17% in C_6D_6
				101.1		97.2		5% in light petroleum[g]
(4d)[h]	Me	63	122—125/0.2	101.8	42/—	97.5	58/—	5% in light petroleum[g]
				103.9	—/8	99.2	—/92	5% in toluene
(4e)	Et	67	100—102/0.2	116.2	72/60	111.6	28/40	15% in C_5D_6
(4f)	Pr^i	45	107/0.4	124.4	58/63	120.6	42/37	10% in toluene
(4g)[i]	Bu^t	47	161—162/1.3	134.8	68/27	130.7	32/73	20% in toluene
				132.6		128.7		5% in light petroleum[g]
				134.9	—/10	130.7	—/90	5% in toluene

[a] n.c. = Not calculated; r.e. = rapid exchange. For compounds (4): initial ratio %/final % after distillation or crystallization; see text. [b] Ref. 1c. [c] ^{31}P-{^{1}H} N.m.r. at 36.43 MHz. [d] ^{31}P-{^{1}H} N.m.r. at 40.48 MHz. [e] Ref. 1d. [f] M.p. for (4c-I), 133 °C. [g] B.p. 30—50 °C. [h] M.p. for (4d-II), 53 °C. [i] M.p for (4g-II), 61 °C.

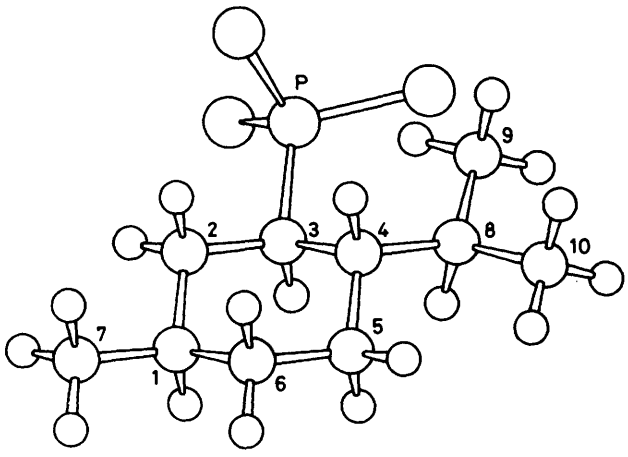

Scheme 3. Numbering of carbons in menthyl skeleton of P(L-men)R(X)Cl (X = S or lone pair)

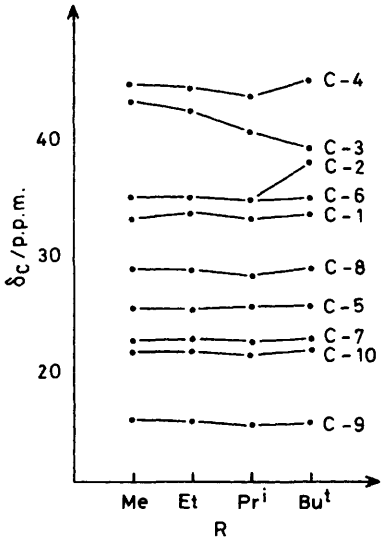

Figure 2. Substituent effects on chemical shifts δ_C in (**2d**)—(**2g**)

(71%), while (**2e-I**) has δ_P = 122.5 p.p.m. (29%). Sulphurisation led to P(L-men)Et(S)Cl epimers (**4e-I**) with δ_P = 116.2 p.p.m. (72%) and (**4e-II**), δ_P = 111.6 p.p.m. (28%). Since n.m.r. arguments deduced (in this paper) the $S_{(P)}$ form for (**4e-II**) the dominant chlorophosphine (**2e-II**) must possess the $R_{(P)}$ configuration. In terms of absolute geometries the major components of (**2c**) and (**2e**), hence the most stable forms, may be described by Scheme 2. This shows clearly that the consistent assignment of a given geometry to the high-frequency resonances does not hold in the phosphine series. Preparative results and chemical shifts are given in Table 1 and Figure 1.

In the next section it is shown that additional evidence for absolute P configurations may be obtained by inspection of specific chemical shifts (δ_C, δ_H) and coupling constants (J_{PC}, J_{PH}), leading to general rules for P-epimeric assignment based solely on n.m.r. data.

Carbon-13 and ^{1}H *N.M.R. Studies at Ambient Temperature.*—(*a*) *General.* Hydrogen-1 n.m.r. spectra were obtained at 200, 360, and 500 MHz. Carbon-13 n.m.r. data resulted from studies at 22.63, 50.29, and 90.52 MHz. Phosphorus-31 chemical shifts were measured by the ^{31}P-{^{1}H} technique at 36.45 MHz. The following spectrometers from Bruker Analytische Messtechnik were used: HX90R, WP200, WP360, and WM500 (operating in the Fourier-transform mode); degassed and sealed samples were employed. Chemical shifts were referenced to internal $SiMe_4$ (δ_H and δ_C) or to 85% H_3PO_4 measured independently as an external reference; δ values are positive for high-frequency shifts.

Table 2. Chemical shifts (δ_C/p.p.m.) and coupling constants (J_{PC}/Hz) for P(L-men)RCl (**2d**)—(**2g**)

R	Me	Et		Pr^i		Bu^t
C-*i*	δ_C[a]	δ_C[a]	δ_C[b]	δ_C[a]	δ_C[b]	δ_C[c]
C-1	33.12	33.77	33.68	33.53	33.10	33.58
C-2	34.94	35.01	34.97	34.97	34.69	37.94
C-3	43.25	42.56	42.23	41.0	40.50	39.13
C-4	44.66	44.65	44.39	44.2	43.62	45.15
C-5	25.34	25.46	25.36	25.40	25.10	25.78
C-6	33.16	33.34	33.68	33.35	33.10	34.96
C-7	22.52	22.55	22.58	22.62	22.42	22.76
C-8	27.82	27.79	27.75	27.52	27.14	27.88
C-9	15.46	15.44	15.37	15.29	15.05	15.40
C-10	21.46	21.49	21.52	21.49	21.28	21.76
P*C*		35.42	33.93	27.69	27.42	33.72
PC*C*		9.18	9.25	19.2	18.91	26.70
				17.0	16.70	
C-*i*	J_{PC}	J_{PC}	J_{PC}	J_{PC}	J_{PC}	J_{PC}
C-1	1.5	0	0	0	0	0
C-2	0.8	0	0	0	0	0
C-3	35.0	37.2	35.6	34	35.4	45.0
C-4	8.6	br	br	br	8.6	17.0
C-5	7.0	6.8	5.2	6.7	6.1	7.7
C-6	2.0	1.7	0	1.2	0	0
C-7	0	0	0	0	0	0
C-8	21.5	21.2	20.6	20.3	17.7	27.3
C-9	2.0	2.0	0	2.1	0	0
C-10	1.0	0.9	0	0	0	0
P*C*		40.4	37.8	30.2	30.3	24.6
PC*C*		19.5	18.9	20	20.2	18.1
				24	22.7	

[a] 50.29 MHz, 70% in C_6D_6–$SiMe_4$. [b] 22.63 MHz, 70% in C_6D_6–$SiMe_4$. [c] 90.52 MHz, 40% in $C_6D_5CD_3$–$SiMe_4$.

(*b*) *Results from* ^{13}C *n.m.r. studies.* Only ten characteristic ^{13}C resonances were observed for the menthyl part of trivalent phosphorus compounds P(L-men)RCl (**2d**)—(**2g**), indicating an exchange process relatively fast on the ^{13}C n.m.r. time-scale. Substituting the smaller methyl group in P(L-men)MeCl (**2d**) by the more bulky t-butyl group in P(L-men)Bu^{t}Cl (**2g**) introduces a substantial high-frequency shift for C-2 and C-4, while C-3 is subjected to a remarkable low-frequency shift. As will be seen from Table 2 and Figure 2 smaller substituent effects are noted for the remaining carbon positions.

The menthyl skeleton in thiophosphoryl chlorides P(L-

Table 3. Chemical shifts (δ_C/p.p.m.) and coupling constants (J_{PC}/Hz) for P(L-men)R(S)Cl (**4d**)—(**4g**)

R	Me[a]		Et[b]		Pr^{i}[c]		Bu^{t}[d]	
C-*i*	δ_C(I)	δ_C(II)	δ_C(I)	δ_C(II)	δ_C(I)	δ_C(II)	δ_C(I)	δ_C(II)
C-1	33.06	33.08	33.12	33.10	33.20	33.16	33.10	32.82
C-2	36.17	35.97	36.20	35.87	36.40	35.80	39.82	37.21
C-3	50.51	50.52	49.23	49.64	46.72	47.38	43.78	43.81
C-4	45.54	43.92	45.50	43.92	45.81	44.34	45.63	44.56
C-5	24.77	24.32	24.76	24.43	25.01	24.58	24.87	24.59
C-6	34.32	34.16	34.19	34.26	34.39	34.32	33.17	33.84
C-7	22.43	22.43	22.49	22.52	22.58	22.56	22.63	22.63
C-8	28.41	27.72	28.45	27.63	28.41	27.45	29.09	27.48
C-9	15.57	15.77	15.84	15.85	16.16	15.91	16.86	16.43
C-10	21.52	21.53	21.51	21.57	21.65	21.61	21.34	21.73
P*C*	31.80	28.70	35.67	33.13	37.76	36.22	45.80	50.57
PC*C*			7.30	6.90	16.74	16.68	25.70	26.24
					16.67	15.65		
C-*i*	J_{PC}(I)	J_{PC}(II)	J_{PC}(I)	J_{PC}(II)	J_{PC}(I)	J_{PC}(II)	J_{PC}(I)	J_{PC}(II)
C-1	14.8	16.8	14.5	16.2	14.2	15.6	12.1	15.6
C-2	4.1	1.3	4.4	1.6	4.4	1.5	4.8	0
C-3	51.1	52.0	48.2	49.6	45.2	46.8	50.5	45.8
C-4	2.2	3.7	2.4	4.0	2.9	4.4	−2	4.3
C-5	14.9	15.4	15.1	14.8	14.4	14.2	13.4	13.3
C-6	2.1	2.2	2.2	2.1	2.2	2.1	0	0
C-7	1.5	1.5	1.0	1.6	0	0	0	0
C-8	3.3	4.5	3.2	4.4	3.1	4.2	2.9	4.5
C-9	0	0	0	0	0	0	0	0
C-10	0	0	0	0	0	0	0	0
P*C*	56.9	60.4	53.5	56.8	50.9	53.7	36.9	42.7
PC*C*			6.4	6.3	3.4	2.1	0	0
					3.2	3.2		

[a] 50.29 MHz, 7% in C_6D_6–$SiMe_4$. [b] 50.29 MHz, 5% in C_6D_6–$SiMe_4$. [c] 50.29 MHz, 12% in C_6D_6–$SiMe_4$. [d] 90.52 MHz, 10% in C_6D_6–$SiMe_4$.

Table 4. Substituent effects on chemical shifts (δ_H/p.p.m.) and vicinal coupling constants ($^3J_{HH}$/Hz) of methyl groups for P(L-men)RCl (**2d**)—(**2g**)

	(**2d**)	(**2e**)	(**2f**)	(**2g**)
R	Me	Et	Pr^{i}	Bu^{t}
CH_3-*i*	δ_H[a]	δ_H[a]	δ_H[a]	δ_H[b]
CH_3-7	0.861	0.876	0.889	0.866
CH_3-9	0.858	0.854	0.900	0.894
CH_3-10	0.778	0.787	0.792	0.711
CH_3-*i*	$^3J_{HH}$	$^3J_{HH}$	$^3J_{HH}$	$^3J_{HH}$
CH_3-7	6.2	6.2	5.5	6.1
CH_3-9	7.3	6.7	6.9	6.8
			0.9[c]	1.0[c]
CH_3-10	6.8	6.8	6.9	6.8

[a] 200 MHz, 5% in C_6D_6–$SiMe_4$. [b] 360 MHz, 4% in $C_6D_5CD_3$–$SiMe_4$. [c] Coupling constants $^5J_{PH}$/Hz.

Table 5. Substituent effects on chemical shifts (δ_H/p.p.m.) and vicinal coupling constants ($^3J_{HH}$/Hz) of methyl groups in P-epimeric forms of P(L-men)R(S)Cl (**4d**)—(**4g**)

		(**4d**)	(**4e**)	(**4f**)	(**4g**)
	R	Me	Et	Pr^{i}	Bu^{t}
CH_3-*i*, H-*i*	Form	δ_H[a]	δ_H[a]	δ_H[a]	δ_H[b]
H-8	I	2.319	2.483	2.745	2.640
	II	2.847	2.866	2.852	2.961
CH_3-7	I	0.774	0.797	0.801	0.785
	II	0.712	0.758	0.781	0.719
CH_3-9	I	0.597	0.697	0.796	0.727
	II	0.833	0.843	0.827	0.856
CH_3-10	I	0.862	0.871	0.902	0.957
	II	0.984	0.977	0.973	0.996
		$^3J_{HH}$	$^3J_{HH}$	$^3J_{HH}$	$^3J_{HH}$
CH_3-7	I	6.3	6.5	6.3	6.4
	II	5.9	6.3	6.1	6.1
CH_3-9	I	6.7	6.8	7.0	6.9
	II	6.8	6.8	6.8	6.9
CH_3-10	I	6.3	6.8	6.6	6.6
	II	6.8	6.8	6.8	6.7

[a] 500 MHz, 5% in C_6D_6–$SiMe_4$. [b] 360 MHz, 10% in C_6D_6–$SiMe_4$.

men)R(S)Cl is more sensitive towards the R substituent size. Exchange of Me for Bu^{t} is connected with a decrease of δ_C for C-3 and C-6, while C-2, C-4, C-8, and C-9 have increased δ_C values. If a descriptive variable $\Delta_i = \delta_{C\text{-}i}$ (form I) − $\delta_{C\text{-}i}$ (form II) is calculated for (**4d**)—(**4g**) from Table 2, substituent-specific effects are seen. The P-epimeric forms I have higher $\delta_{C\text{-}i}$ values for C-2, C-4, C-5, and C-8. The parameter Δ_i increases for C-2 and C-9, but decreases for C-4 and C-6 in a monotonic fashion for the substitution series R = Me → Et → Pr^{i} → Bu^{t} in (**4d**)–(**4g**). The trends described above are shown in Figure 3.

Phosphorus–carbon coupling constants may also serve as indicators for configuration at phosphorus and molecular conformation of model systems including menthyl substituents. The vicinal J_{PC} couplings in trivalent phosphorus compounds (**2a**)–(**2g**) behave in a typical 'anti-Karplus' fashion: $^3J^{t}_{PC\text{-}i}$ is smaller than $^3J^{g}_{PC\text{-}j}$ (i = 1 or 5, j = 8; t = *trans*, g = *gauche*). The opposite holds for the five-valent thiophosphoryl derivatives (**4a**)—(**4g**), as may be derived from Tables 2 and 3. This is consistent with findings from norbornylphosphorus compounds.[8] While $^3J^{t}_{PC\text{-}1} \ll {}^3J^{t}_{PC\text{-}5}$ or is *ca.* zero in (**1**) and (**2a**)—

(**2g**), an interesting cross-rule exists for (**4c**)—(**4d**) (see Figure 4): $^3J^t_{PC\text{-}1} < {}^3J^t_{PC\text{-}5}$ only for the P-epimeric form **I**, while $^3J^t_{PC\text{-}1} > {}^3J^t_{PC\text{-}5}$ in form **II**. In addition, the P-epimers may be differentiated by $^3J^g_{PC\text{-}8}$: form **I** shows smaller values than form **II**.

Table 6. Chemical shifts (δ_H/p.p.m.) and coupling constants $^3J_{HH}$, $^2J_{PH}$, and $^3J_{PH}$ (Hz) from partial analysis of ^{1}H n.m.r. spectra: alkyl groups R in P-epimeric forms of P(L-men)R(S)Cl (**4d**)—(**4g**)

			PCH*		PCCH		
	R	Form	δ_H	$^2J_{PH}$	δ_H	$^3J_{PH}$	$^3J_{HH}$
(**4d**)	Me	I	1.804	11.9			
		II	1.614	12.5			
(**4e**)	Et	I	n.a.		1.218	22.6	7.4
		II			1.131	22.2	7.4
(**4f**)	Pr^i	I			0.869	20.4	6.8
					1.128	21.4	6.9
		II	n.a.		1.271	21.0	6.8
					1.125	20.4	6.7
(**4g**)	Bu^t	I			1.192	19.5	
		II			1.245	18.5	

* n.a. = Not assigned.

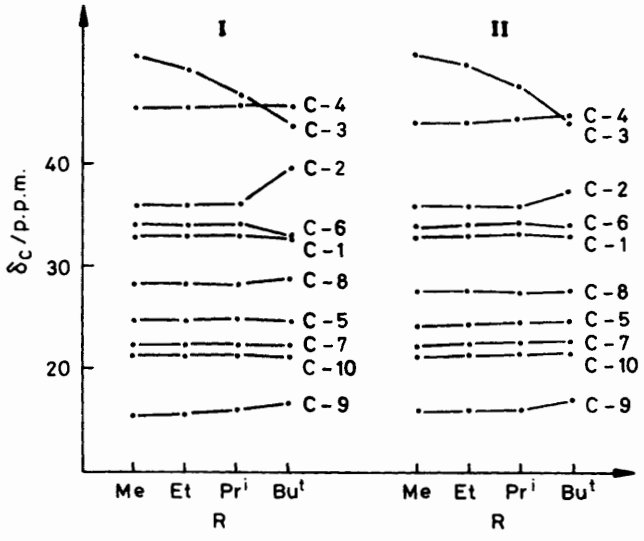

Figure 3. Substituent effects on chemical shifts δ_C in P-epimeric forms of (**4d**)—(**4g**)

The geminal phosphorus–carbon coupling constants $^2J_{PC\text{-}2}$ and $^2J_{PC\text{-}4}$ proved to be of high diagnostic value when assigning the absolute configuration to phosphorus in compounds of the type P(L-men)R(S)Cl. Another useful cross-rule holds for (**4c**)—(**4g**): $^2J_{PC\text{-}2}$ is greater in form **I** than in form **II**; the opposite is true for $^2J_{PC\text{-}4}$. In addition, $^2J_{PC\text{-}2} > {}^2J_{PC\text{-}4}$ for form **I**, and again the reversed statement holds for form **II**. In thiophosphoryl chlorides (**3**) and (**4a**)—(**4g**) typical values for $^2J_{PC}$ range between 0 and 5 Hz. In contrast, the chlorophosphines exhibit $^2J_{PC\text{-}2}$ *ca.* 0 and $^2J_{PC\text{-}4}$ 7—19 Hz.

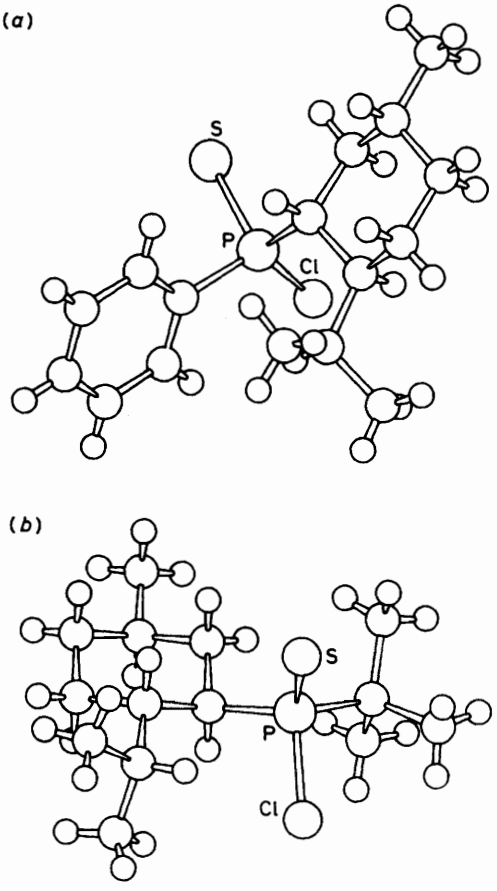

Figure 5. Solid-state structures from *X*-ray diffraction studies on P(L-men)R(S)Cl:[1d,e] (*a*) (**4c-I**), R = Ph; (*b*) (**4g-II**), R = Bu^t

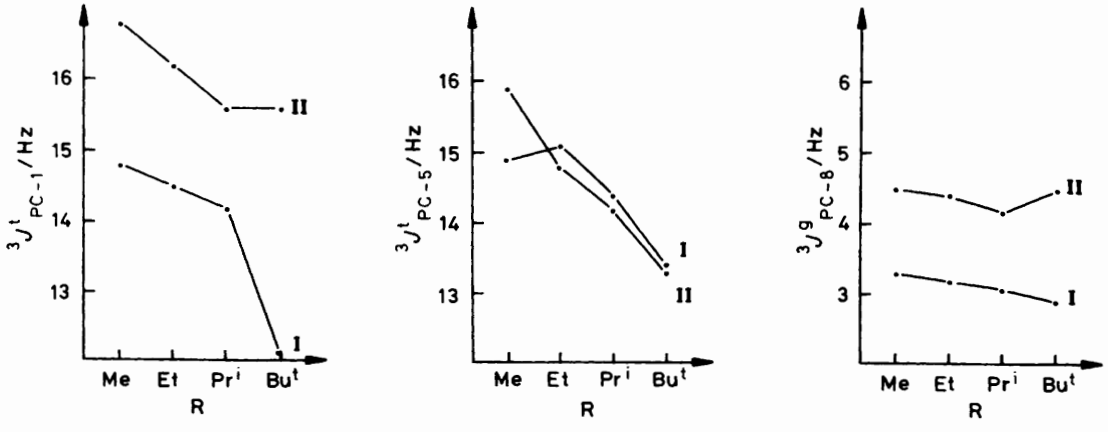

Figure 4. Substituent effects on vicinal coupling constants $^3J_{PC}$ in P-epimeric forms of (**4d**)—(**4g**)

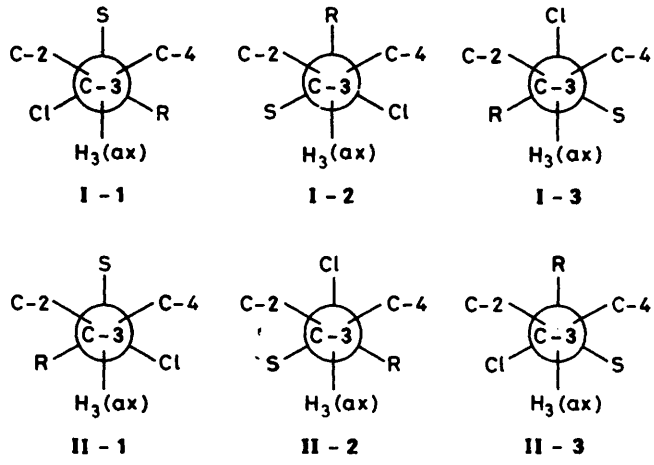

Scheme 4. Three classical rotamers for both P-epimers of P(L-men)R(S)Cl (**4**)

It is known from independent research[9] that geminal coupling constants $^2J_{PC}$ reflect the relative orientation of lone pairs or electronegative substituents connected to phosphorus in chains like X–P–C–C (X = lone pair or halogen): if X is *trans* to C, smaller values of $^2J_{PC}$ are observed than for *gauche* conformations.[10] Thus, for forms **I** of P(L-men)R(S)Cl the chlorine should be oriented *trans* towards C-4, whereas in form **II** it is presumably preferably *trans* with respect to C-2. This conclusion is fully supported by our *X*-ray studies of (**4c-I**) [$S_{(P)}$][1d] and (**4g-II**) [$R_{(P)}$],[1e] as given in Figure 5.

It is tempting to suggest that the lone pair in chlorophosphines might be oriented *trans* to C-2, but the relevant ^{13}C n.m.r. observations are results from exchanging systems, as will be discussed below.

Long-range coupling constants $^4J_{PC}$ were detected, again decreasing with substituent size. While splittings due to $^4J_{PC\text{-}6}$ in methyl-, ethyl-, and isopropyl-substituted chlorophosphines (**2d**)—(**2f**) and in the thio derivatives (**4d**)—(**4f**) were resolved within 1.2—2.0 Hz, the spectra of the methyl groups bound to the menthyl skeleton revealed a controversial behaviour. In trivalent phosphorus compounds (**2d**) and (**2e**) $^4J_{PC\text{-}7}$ was undetectably small, but in thiophosphoryl chlorides (**4d**) and (**4e**) couplings were resolved and were found to be *ca.* 2 Hz. In contrast CH_3-9 and CH_3-10 have couplings to trivalent phosphorus in (**2d**) and (**2e**) of 0.9—2.0 Hz, while the corresponding compounds (**4d**) and (**4e**) of pentavalent phosphorus show no sign of resolvable couplings. Substitution of R in P(L-men)-R(S)Cl by Me → Et → Pr^i induces a generally monotonic variation in n.m.r. parameters, which might be explained in simple terms as a result of increasing demands of substituent volume. However, some remarkable deviations from expectation are seen for $\delta_{C\text{-}2}$, $\delta_{C\text{-}6}$, $^3J_{PC\text{-}1}$, $^3J_{PC\text{-}8}$, $^2J_{PC\text{-}2}$, $^2J_{PC\text{-}4}$, $\delta_{H\text{-}8}$ (form **I**), and $\delta_H(CH_3\text{-}9)$ (form **I**) when adding P(L-men)Bu^t(S)Cl to that series. It is likely that all n.m.r. parameters mentioned above are sensitive towards intramolecular rotation with respect to the $P\text{–}C_{menthyl}$ bond. Therefore, analogous P-epimers from type **I** might prefer individual rotameric forms as a result of steric strain, depending on the size of R. Three classical rotamers may be drawn for each P-epimer, as given in Scheme 4.

While the solid-state conformation of (**4g-I**) comes close to the rotamer **I-1**, the sterically corresponding ring 2[1b,c] of P(L-men)$_2$(S)Cl is similar to rotamer **I-3**. Ring 1[1b,c] of P(L-men)$_2$(S)Cl prefers a situation close to rotamer **II-1**, like (**4g-II**). Based on $^2J_{PC}$ arguments we conclude that P-epimers **I** of (**4d**)—(**4g**) will certainly not occupy rotamers **I-1** or **I-2** but prefer geometries like distorted **I-3** forms. The P-epimers **II** for methyl, ethyl, and isopropyl compounds (**4d**)—(**4f**) will not have rotameric structures **II-1** or **II-3** but prefer **II-2**, in contrast to (**4g-II**) which takes up **II-I** in the solid state. We are continuing *X*-ray studies on P(L-men)R(S)Cl models to reflect n.m.r. parameters which are not fully understood at present.

Additional attention should be directed towards the n.m.r. data of substituents R in compounds (**2**) and (**4**). No simple rule exists to explain the chemical shifts of α-carbons in R from the chlorophosphines (**2d**)—(**2g**). However, for the thiophosphoryl chlorides (**4d**)—(**4g**), $\delta_C(PC_\alpha)$ increases with the number of β-methyl groups, as is the case for the PRR′(S)Br series.[11]

(*c*) *Results from* ^1H *n.m.r. studies.* The menthyl groups in compounds (**2**) and (**4**) give rise to complex ^1H n.m.r. spectra with considerable second-order effects even for high-field measurements. No full two-dimensional n.m.r. treatment on those systems is completed up to now, but the data accessible from direct analyses are significant for stereochemical assignments, and consequently are presented in Tables 4 and 5. Methyl groups CH_3-7, CH_3-9, and CH_3-10 were identified using our two-dimensional n.m.r. studies on P(L-men)Cl_2,[1a] P(L-men)(S)Cl_2,[1b] P(L-men)$_2$(S)Cl,[1b,c] and the pseudo-P-epimeric pair of P(L-men)(D-men)(S)Cl.[1b] In addition, data for protons in alkyl groups R of P(L-men)R(S)Cl are included with Table 6. The following ^1H n.m.r. parameters proved to be stereosensitive indicators. The δ values of H-8 and methyl groups CH_3-9 and CH_3-10 are lower for forms **I** than for **II** in (**4d**)—(**4g**), while the opposite conclusion for CH_3-7 may be drawn from the data in Table 5.

For both P-epimeric forms **I** and **II** the resonances from CH_3-9 are found at lower frequency than those of CH_3-10, a statement which is valid for all substituents R in (**4d**)—(**4g**). The *pro*-R methyl group CH_3-9, which is situated closer to the phosphorus centre than the *pro*-S group CH_3-10, is the more sensitive to substituent effects. Thus an expression $\Delta = \delta_H(CH_3\text{-}9) - \delta_H(CH_3\text{-}10)$ will decrease with increasing size of R in P(L-men)R(S)Cl. No simple rule could be found to pre-estimate the chemical shifts of methyl groups in (**2d**)—(**2g**), but some surprising long-range couplings $^5J_{PH}$ were found for CH_3-9 in P(L-men)RCl with R = Pr^i or Bu^t, but not in any other of the compounds in the series (**2d**), (**2e**), and (**4d**)—(**4g**). It is a useful hypothesis to consider through-space interactions between phosphorus lone pairs and proximal methyl protons as a possible source of a coupling contribution. Proton data (as far as accessible) for alkyl groups R are consistent with findings for PRR′(S)Br compounds. It is straightforward to compare the methyl and t-butyl groups attached directly to phosphorus in (**4d**) and (**4g**). A cross-rule may be formulated leading to a clear distinction of P-epimeric forms: $\delta_H(PMe\text{-}I) > \delta_H(PMe\text{-}II)$, $\delta_H(PCMe\text{-}I) < \delta_H(PCMe\text{-}II)$, $|^2J_{PMe\text{-}I}| < |^2J_{PMe\text{-}II}|$, $^3J_{PCMe\text{-}I} > {}^3J_{PCMe\text{-}II}$.

(*d*) *Conclusions.* P-Epimeric forms of P(L-men)R(S)Cl may be identified using chemical shift values for carbon atoms C-4 and C-8, protons H-8, CH_3-7, CH_3-9, and CH_3-10 and coupling constants $^2J_{PC\text{-}2}$, $^2J_{PC\text{-}4}$, $^3J_{PC\text{-}1}$, and $^3J_{PC\text{-}8}$. Using the stereochemical rules described in this report, we were able to identify the absolute configuration of phosphorus atoms in X(L-men)RP–PR(L-men)Z and X(L-men)RP–S–PR(L-men)Z structures (X, Z = lone pair or S) without *X*-ray analysis, as will be reported in forthcoming papers. Interpretation of n.m.r. data from P(L-men)RCl in the solution state is much more difficult, since dynamic systems with halogen-exchange reactions are involved, as described in the following section.

Exchange Studies on Chlorophosphines by N.M.R. Methods.—(*a*) *General.* Trivalent phosphorus halogen compounds are subject to homo- and hetero-halogen exchange processes as shown in equation (5) (R^1—R^4 = halogen, alkyl, or aryl; X,

$$R^1R^2PX + R^3R^4PY \longleftrightarrow R^1R^2PY + R^3R^4PX \quad (5)$$

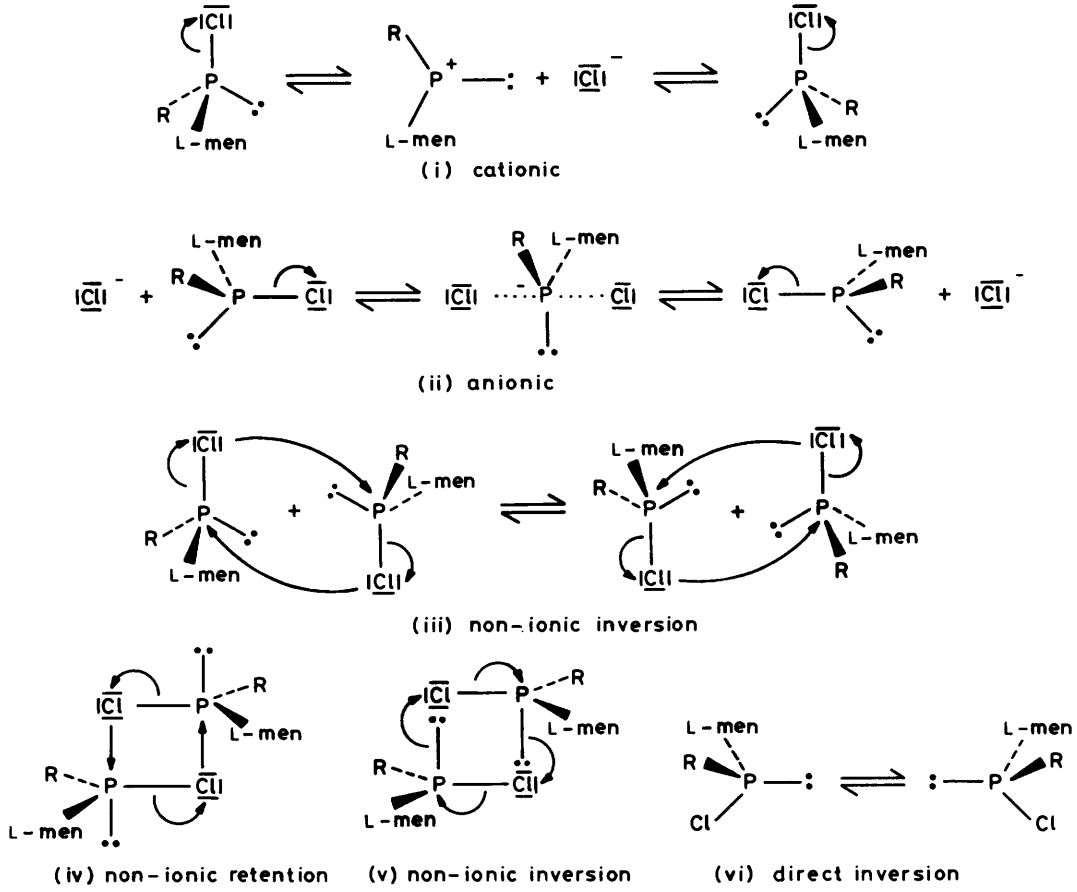

Y = F, Cl, Br, or I). An increase of reaction rate has been observed with increasing size of halogens X and Y.[12]

Ionic and non-ionic mechanisms may be discussed to explain the experimental evidence. The homo-halogen exchange in P(L-men)RCl (R = Et or Ph) may be described by five different mechanisms, (i)—(v). Of these, mechanisms (i) and (ii) proceed *via* cationic or anionic intermediates, which reform neutral chlorophosphines and lead to racemisation. Of the non-ionic (transient dimerisation) routes, mechanisms (iii) and (v) cause inversion of configuration whereas mechanism (iv) involves retention (which would not be detected by n.m.r.). However, it is clear that, to discuss n.m.r. effects, both ionic and non-ionic contributions to an overall mechanism should be taken into account. In principle, direct inversion [mechanism (vi)] also needs to be considered. N.m.r. spectra of solutions of (**2c**) show remarkable solvent effects which are not consistent with direct inversion. Thus, while solutions in $CDCl_3$ have sharp resonance lines in the ^{13}C-$\{^1H\}$ n.m.r. spectra, broad lines occur for carbons C-2, C-4, and C-8 when aromatic solvents like C_6D_6 or $C_6D_5CD_3$ are used. ^{31}P-$\{^1H\}$ N.m.r. spectra of (**2c**) in $CDCl_3$ simply show a single line, while C_6D_6 or $C_6D_5CD_3$ solvents cause separate discrete signals to appear for both P-epimeric forms having either $R_{(P)}$ or $S_{(P)}$ configuration. Addition of NBu^n_4Cl to the latter solutions causes coalescence, thus indicating a fast halogen-exchange reaction promoted by chloride ion. Moreover, heating a solution of pure (**2c**) in aromatic solvents (in the absence of additional chloride ions) leads to the merging of individual ^{31}P-$\{^1H\}$ n.m.r. signals.

To study further halogen exchange in chlorophosphines, we subjected the readily available ethyl and phenyl derivatives (**2e**) and (**2c**) to lineshape and selective inversion-recovery techniques in ^{31}P n.m.r. (see below).

The missing members of the series P(L-men)RCl with R = Me or Pr^i are less suitable for kinetic studies to be performed with present technology but will be investigated in future. The methyl compound (**2d**) undergoes fast exchange, showing a ^{31}P-$\{^1H\}$ singlet with a spectral half-width of 3.7 Hz at 25 °C, broadening to 9.4 Hz on cooling to −17 °C. The P-epimer specific resonances did not split within the temperature range investigated.

Variable-temperature ^{31}P-$\{^1H\}$ n.m.r. studies on (**2f**) reveal a rather intricate pattern which is not understood at present. At −17 °C a single line is detected which broadens on warming to 25 °C, to narrow again at 70 °C. A combination of P–C rotations and halogen-exchange processes probably gives rise to the unexpected behaviour. No attempts were made to analyse the temperature dependence of ^{31}P-$\{^1H\}$ n.m.r. spectra of the t-butyl compound (**2g**), which shows a single line at 36.43 MHz at ambient temperature. This more bulky compound has some similarity to P(L-men)$_2$Cl (**2a**) and P(L-men)(D-men)Cl (**2b**), which undergo fast halogen exchange, as deduced from ^{13}C n.m.r.

(*b*) *N.m.r. methods.* Exchange reactions can be studied, using n.m.r., by different methods, depending on the rate of reaction. For example, if the rate of reaction is of the order of the difference in resonance frequency between the species involved, and if the reaction occurs during the free induction decay, the lineshapes will be affected. If the relaxation rates are known, and the lines are not broadened by other factors, a bandshape analysis can be carried out. A simulated bandshape is fitted to the experimental bandshape by varying the rate constant for the reaction. If the experiment can be done over a wide range of temperatures, this method is accurate. A computer program for solving the relevant two-site exchange equation (uncoupled

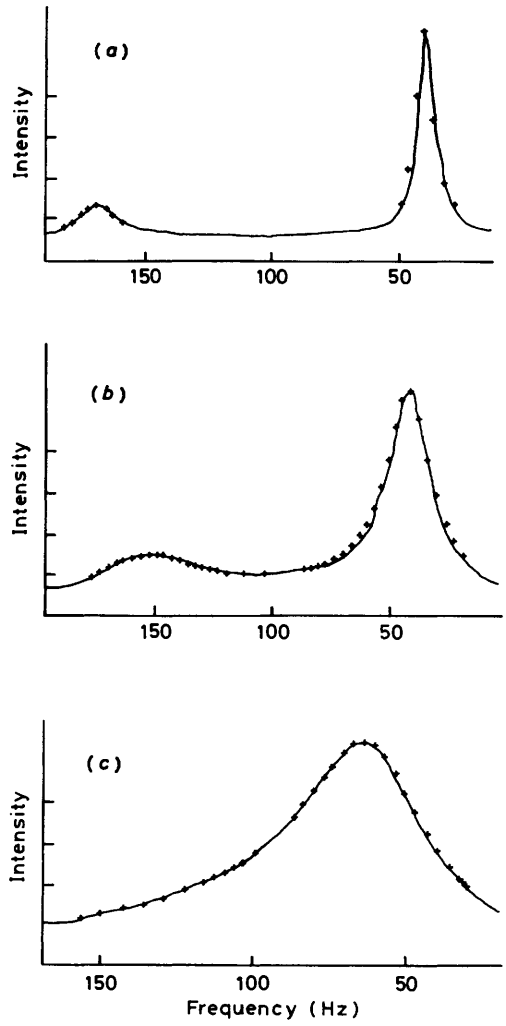

Figure 6. Digitized experimental ^{31}P-{^{1}H} n.m.r. bandshape (+), with computer simulations (—) for (**2e**) at (*a*) 259, (*b*) 285, and (*c*) 317 K. The frequency scales are with respect to an arbitrary zero

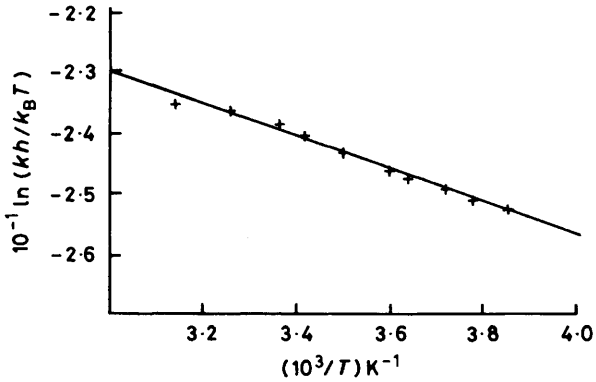

Figure 7. Eyring plot of exchange rates for the process (**2e-I**) (high δ_P) ⟶ (**2e-II**) (low δ_P), as deduced from ^{31}P-{^{1}H} n.m.r. bandshape studies

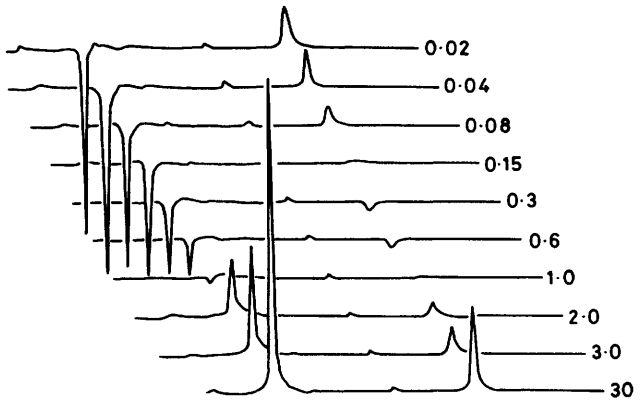

Figure 8. Selective inversion-recovery ^{31}P-{^{1}H} n.m.r. spectra for (**2c**) at 3 °C. The recovery interval (s) is indicated beside each spectrum

system with unequal populations) was written in BASIC for the APPLE II computer. This program iteratively fits the chemical shifts ν_1 and ν_2, the linewidth parameter $\Delta\nu_{\frac{1}{2}}$ (linewidth at half-height in the absence of exchange), the populations p_1 and p_2, and the rate constant for the forward direction, k, to an n.m.r. bandshape broadened by chemical exchange.

For reactions where the rate is too slow to affect the bandshapes, or if the lines are broadened by other factors, *e.g.* relaxation induced by paramagnetic species, other methods have to be used in order to study exchange.

In the case of pulsed n.m.r., a method using selective inversion of one nucleus is specially suitable.[13] If the species with the inverted nuclei is exchanging with other species, negative magnetization may be transferred before relaxation is complete. If the system is monitored with a 90° pulse at time τ after the selective pulse, the intensities for the non-inverted peaks will therefore be reduced, and the inverted peak will recover faster than if there were no exchange. By doing the experiment for different times τ, and fitting a set of theoretical, simulated data to the experimental data, the rate constants for the exchange can be determined. A program was written[14] in BASIC for the APPLE II computer to simulate the results of selective inversion experiments using the equations involving two-site chemical exchange published by Campbell *et al.*[13] This program iteratively fits T_1 values for each site, the populations p_1 and p_2, and the rate constant for the forward direction, k, to the fraction of equilibrium z-magnetization for the exchanging nuclei being observed.

The pulse sequence described in refs. 15 and 16 has been used here for selective inversion. The method consists of a regular sequence of n short identical pulses with a 'tip angle' making up a 180° pulse. In the interval (τ_1) between the pulses, each magnetization vector precesses through an angle $\theta = 2\pi\tau_1\Delta f$ radians, Δf being the offset from f_o, the carrier frequency. Now if θ is set to $\theta = 2\pi n$, *i.e.* $\Delta f = n/\tau_1$, the pulse will have a cumulative tipping effect of the vector towards the negative z-axis. For all other offsets the overall flip angle will be small. As in normal inversion-recovery experiments a 90° observation pulse is applied at time τ_2 after the selective 180° pulse.

(*c*) *Experiments on* (**2e**) *and* (**2c**). A 70% solution of (**2e**) in C_6D_6 and a 30% solution of (**2c**) in $C_6D_5CD_3$ were prepared by the usual techniques and examined using a JEOL FX100 spectrometer operating at 40 MHz for ^{31}P n.m.r. with complete decoupling of protons. Rate constants were evaluated for sample (**2e**) by performing bandshape analyses on ^{31}P-{^{1}H} n.m.r. exchange-broadened spectra obtained at ten different temperatures over the range 259—317 K. Spectra were obtained using a pulse duration of 10 μs, corresponding to a flip angle of 69°, and an acquisition time of 5.85 s, a spectral width of 1 400 Hz, 10 transients, and a pulse delay of 15 s. Calculations were performed using the computer program mentioned above.

For sample (**2c**) rate constants were deduced from selective

inversion-recovery experiments using $^{31}P-\{^1H\}$ n.m.r. spectra obtained at five different temperatures over the range 268—320 K. The selective 180° pulse was made up of 12 minipulses with duration of 3.0 μs, and a delay between minipulses of 3.35—3.6 ms. These minipulses were followed by a 90° pulse of duration 13 μs. The spectra were obtained using an acquisition time of 2.24 s, and a spectral width of 800 Hz, 100 transients, a pulse delay of 30 s, and 10 different pulse intervals for each temperature, with a 30 s pulse-interval spectrum used as a reference. The reference spectrum was integrated for each temperature and the relative amount of the epimers calculated. The exchange rates were evaluated using the computer program mentioned above.

For both compounds thermodynamic activation parameters were calculated according to the Eyring theory. The $\Delta H^{\ddagger}$ and $\Delta S^{\ddagger}$ values were obtained from a least-squares treatment of the corresponding rate data. Equilibrium constants were obtained from the data-fitting process in the bandshape and selective inversion-recovery experiments. The thermodynamic parameters for the reactions were obtained from a least-squares treatment of equilibrium constants according to the van't Hoff relationship.

Table 7. Rate constants (k) and equilibrium constants (K) for the inversion of P(L-men)EtCl (**2e**)

T/K	k/s^{-1} (**2e-II**) → (**2e-I**)	K [(**2e-II**)]/[(**2e-I**)]
259	23	
264	26	2.60
268	31	2.61
274	40	2.48
277	46	2.51
285	68	2.29
292	99	2.19
296	123	2.17
306	164	2.08
317	190	2.07

Table 8. Rate constants (k) and equilibrium constants (K) for the inversion of P(L-men)PhCl (**2c**)

T/K	k/s^{-1} (**2c-I**) → (**2c-II**)	K [(**2c-I**)]/[(**2c-II**)]
268	1.2	2.78
276	2.25	2.70
295.5	6.7	2.44
305	7.5	2.22
320	20	2.13

Discussion

Figure 6 shows the experimental bandshapes, together with the computer simulations, for (**2e**) at three temperatures. The equilibrium constants and first-order rate constants for (**2e**) are given in Table 7. Figure 7 illustrates the Eyring plot for the exchange (**2e-I**) → (**2e-II**).

Figure 8 shows one of the sets of spectra obtained from $^{31}P-\{^1H\}$ selective inversion-recovery experiments on (**2c**). It can be seen how negative magnetization is transferred from the inverted peak to the non-inverted peak during the recovery. Calculated and experimental plots for the experiment at 276 K are shown in Figure 9. The equilibrium constants and first-order rate constants for the exchange (**2c-I**) → (**2c-II**) are listed in Table 8, and the equilibrium data to obtain the thermodynamic parameters are plotted in Figure 10.

The enthalpy, entropy and free energy for the equilibrium, together with the enthalpy, entropy and free energy of activation, obtained from least-squares fits to the data, are given for both compounds in Table 9. For the Eyring plots the transmission coefficient for the exchange has been set to unity. For all the data the exchange direction (more stable form) → (less stable form) has been used.

Under the assumption that the high-frequency resonance corresponds to the $S_{(P)}$ configuration in each case, it is clear that there is an almost exact reversal of relative stability of the two forms **I** and **II** between (**2e**) and (**2c**). As shown in Scheme 2, however, this corresponds to similar stabilities for analogous configurations, though the epimeric labels $S_{(P)}$ and $R_{(P)}$ are inconsistently related to configuration.

Table 9. Thermodynamic parameters for reaction and activated complex formation for the inversion reaction of (**2c**) and (**2e**) (estimated deviations in parentheses). In each case the data are given for the direction (more stable form) → (less stable form). For (**2e**) this is **II** → **I** (low δ_P → high δ_P), whereas for (**2c**) it is **I** → **II** (high δ_P → low δ_P)

	(**2e**)	(**2c**)
ΔH of reaction/kJ mol^{-1}	3.5 (0.3)	3.8 (0.3)
ΔS of reaction/J K^{-1} mol^{-1}	5.4 (0.4)	5.8 (0.2)
ΔG of reaction/kJ mol^{-1} at 298 K	1.9	2.1
$\Delta H^{\ddagger}$ of activation/kJ mol^{-1}	25.7 (0.9)	33.9 (2.8)
$\Delta S^{\ddagger}$ of activation/J K^{-1} mol^{-1}	−119.1 (0.6)	−115.3 (1.4)
$\Delta G^{\ddagger}$ of activation/kJ mol^{-1} at 298 K	61.2	68.2

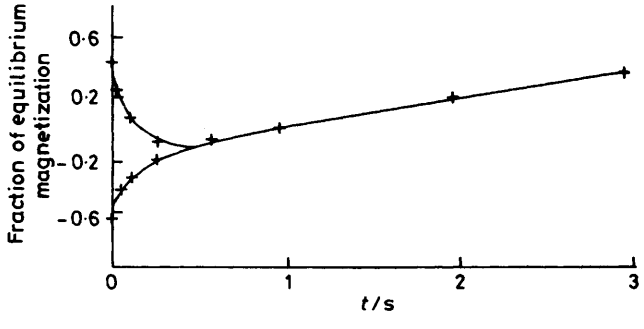

Figure 9. Calculated (—) and experimental (+) plots for the selective inversion-recovery $^{31}P-\{^1H\}$ n.m.r. experiments on (**2c**) at 3 °C (see Figure 8)

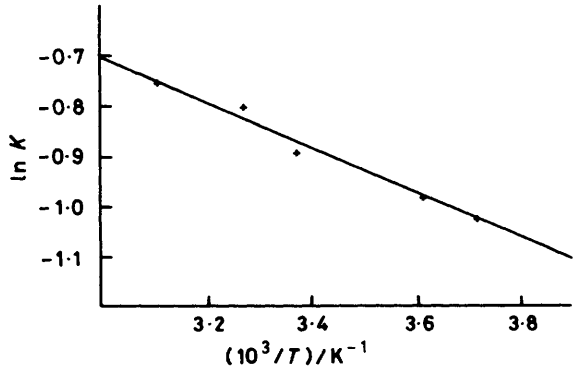

Figure 10. Plot of equilibrium ratios [(**2c-II**)]/[(**2c-I**)] = K (in logarithmic form), based on ^{31}P n.m.r. data, *vs.* inverse temperature. Form **I** is the one giving the signal at higher δ_P

The enthalpy of activation for the phenyl compound is substantially higher than that for the ethyl system. This is contrary to expectation since the effects of substituent bulk should destabilise the ground state for (**2c**) whereas resonance effects would be expected to stabilise any planar activated state. The entropy of activation for both reactions is high, the two values being within 4% of one another. Of course, determination of $\Delta S^{\ddagger}$ by individual n.m.r. methods is well known to be subject to systematic error (so that $\Delta G^{\ddagger}$ for the middle of the temperature range studied is the most accurate activation parameter). However, a high value of $\Delta S^{\ddagger}$ is consistent with the suggestion that inversion is a two-step reaction, where chlorine is abstracted in the first step and attack at phosphorus in the second step forms either of the two possible configurations. These results favour a mechanism *via* cationic intermediates [mechanism (i)]. It should be noted that since this mechanism involves racemisation rather than inversion, the true rate of the process is twice the rate observed by n.m.r.: this factor is incorporated into $\Delta S^{\ddagger}$. The alternatives [mechanisms (ii), (iii) and (v)] are discarded, as is classical pyramidal inversion at phosphorus. Experimental evidence on tris-substituted phosphines [17] and theoretical considerations show that the barrier to direct pyramidal inversion at phosphorus is far too high to account for the dynamic effects observed and described above. However, as far as we are aware, the literature does not contain data on inversion kinetics for halogenophosphine compounds.

In conclusion, we wish to point out that introducing a chiral n.m.r. probe (a menthyl ligand) into chlorophosphines yields a convenient route to kinetic data which is inaccessible for achiral model systems.

Experimental

(*a*) *General.*—The following compounds were obtained according to literature methods: (L-men)Cl,[18] Mg(L-men)Cl,[5] $MgPr^{i}Cl$,[19] $MgBu^{t}Cl$,[19] (**1**),[4] (**2a**)—(**2c**), (**2g**), (**4a**)—(**4c**), (**4g**),[20,1b,1d,1e] (**3**).[20,1b] The compounds $PMeCl_2$, $PEtCl_2$, and l-menthol were obtained from industrial sources. All operations were carried out under dry N_2 and with dry solvents.

(*b*) *Chloro*(L-*menthyl*)*methylphosphine,* (**2d**).—A solution of $PMeCl_2$ (115.7 g, 0.99 mol) in diethyl ether (600 cm^3) was maintained at between −50 and −30 °C. Within 3 h Mg(L-men)Cl (1.1 mol) in thf (900 cm^3) was added with stirring. After addition, the reaction mixture was allowed to warm up to room temperature followed by refluxing for 0.5 h. Pyridine (50 cm^3) was added at room temperature. The precipitate was filtered off using a Schlenk tube and washed with ether (5 × 100 cm^3). Solvents were distilled off from the combined organic phases using a Vigreux column (30 cm). Fractional distillation with a Zincke apparatus yielded 122.5 g (56%) of (**2d**), b.p. 78—80 °C (0.2—0.3 Torr) (Found: Cl, 16.0; P, 13.9. Calc. for $C_{11}H_{22}ClP$: Cl, 16.05; P, 14.05%); δ_P (pure) 108.9 p.p.m.

(*c*) *Chloroethyl*(L-*menthyl*)*phosphine,* (**2e**).—An analogous procedure to that in (*b*) was used: $PEtCl_2$ (131.0 g, 1.0 mol), ether (600 cm^3), −40 to −20 °C, Mg(L-men)Cl (1.5 mol) in thf (680 cm^3), 3 h; yield 149.3 g (64%), b.p. 95 °C (0.2 Torr) (Found: Cl, 14.9; P, 12.85. Calc. for $C_{12}H_{24}ClP$: Cl, 15.1; P, 13.2%); δ_P (pure) = 122.5 (**I**, 29%), 119.9 p.p.m. (**II**, 71%).

(*d*) *Chloroisopropyl*(L-*menthyl*)*phosphine,* (**2f**).—P(L-men)Cl_2 (41.4 g, 0.17 mol) was dissolved in ether (500 cm^3). At −30 to −20 °C, a solution (53 cm^3) of $MgPr^{i}Cl$ (3.2 molar in ether) was added under stirring within 3 h. After the addition was complete the system was maintained for 1 h at −30 °C and 1 h at room temperature. After filtration, solvents were driven off using a Vigreux column. Fractional distillation using a column (10 cm) packed with Raschig rings led to a yield of 19.0 g (45%) of (**2f**), b.p. 112.9 °C (0.4 Torr) (Found: Cl, 14.15; P, 12.35. Calc. for $C_{13}H_{26}ClP$: Cl, 14.25; P, 12.45%); δ_P (pure) = 124.5, δ_P (5% in thf) = 124.7 (**I**, 30%), 121.4 p.p.m. (**II**, 70%).

(*e*) L-*Menthyl*(*methyl*)*thiophosphoryl Chloride,* (**4d**).—To (**2d**) (9.8 g, 0.044 mol) a solution of sulphur (2.0 g, 0.062 mol) in CS_2 (100 cm^3) was added. CS_2 was driven off slowly and the remaining mixture was heated to 180 °C. After cooling to room temperature light petroleum (b.p. 30—50 °C, 40 cm^3) was added. Excess sulphur was filtered off; P-enantiomeric ratio in solution, **I**/**II** = 42/58. Crystallization at −110 °C led to 7.1 g (63%) of (**4d**). Repeated fractional crystallization leads to 1.7 g (**4d**) pure form **II**. Distillation of the reaction mixture leads to (**4d**), **I**/**II** = 42/58, b.p. 122—125 °C (0.2 Torr) (Found: Cl, 13.6; S, 12.8. Calc. for $C_{11}H_{22}ClPS$: Cl, 14.0; S, 12.7%); δ_P (5% in light petroleum) = 101.8 (**I**, 42%), 97.5 (**II**, 58%), δ_P (5% in C_6D_6) = 99.4 p.p.m. (pure **II**).

(*f*) *Ethyl*(L-*menthyl*)*thiophosphoryl Chloride,* (**4e**).—An analogous procedure to that in (*e*) was used: (**2e**) (12.2 g, 0.05 mol), sulphur (1.6 g, 0.05 mol), $AlCl_3$ (0.1 g), light petroleum (b.p. 100—140 °C, 40 cm^3), 4 h reflux; yield 9.3 g (67%), b.p. 100—102 °C (0.2 Torr) using a Kugelrohr-distillation, viscous oil (Found: Cl, 13.0; S, 12.4. Calc. for $C_{12}H_{24}ClPS$: Cl, 13.3; S, 12.0%); δ_P (15% in C_6D_6) = 116.2 (**I**, 60%), 111.6 p.p.m. (**II**, 40%).

(*g*) *Isopropyl*(L-*menthyl*)*thiophosphoryl Chloride,* (**4f**).—A mixture of (**2f**) (8.7 g, 0.035 mol) and sulphur (1.1 g, 0.038 mol) was warmed up to 140 °C and maintained for 4 h at this temperature. The cold reaction mixture was dissolved in light petroleum (b.p. 30—50 °C, 40 cm^3) and excess sulphur was filtered off. The remaining solution yielded, after distillation, 19.0 g (45%) of colourless oil, b.p. 107 °C (0.4 Torr) (Zincke-apparatus) (Found: P, 11.0; S, 11.4. Calc. for $C_{13}H_{26}ClPS$: P, 11.0; S, 11.4%); δ_P (10% in toluene) = 124.4 (**I**, 63%), 120.6 p.p.m. (**II**, 37%).

Acknowledgements

We thank the Ministerium für Wissenschaft und Forschung des Landes Nordrhein-Westfalen, Fonds der Chemischen Industrie (G. H.) the S.E.R.C. (R. K. H.) for grants, and N.A.T.O. for a travel grant. Dr. D. Wendisch (Bayer AG, Leverkusen) and Dr. H. Schneiders (Bruker Analytische Meßtechnik GmbH, Rheinstetten) provided additional n.m.r. spectra using 360- and 500-MHz spectrometers; Dr. R. Wagner (Henkel KGaA, Düsseldorf) assisted with the WP200 spectra; Hoechst AG, Knapsack-Hürth and Haarman & Reimer, and Holzminden, supplied starting chemicals. One of us (P. T. J.) thanks EKA AB for financial support, and C. J. C. is grateful to Hamline University for provision of Study Leave.

References

1 (*a*) Part 1, M. Feigel, G. Hägele, A. Hinke, and G. Tossing, *Z. Naturforsch., Teil B,* 1982, **37**, 1661; (*b*) Part 2, G. Hägele, W. Kückelhaus, J. Seega, G. Tossing, H. Kessler, and R. Schuck, *ibid.*, 1985, **40**, 1053; (*c*) Part 3, R. Boese, G. Hägele, W. Kückelhaus, J. Seega, G. Tossing, and H. Schneiders, *Phosphorus Sulfur,* 1986, **28**, 351; (*d*) Part 4, R. Boese, G. Hägele, W. Kückelhaus, J. Seega, and G. Tossing, *Chem. Zeitung,* 1985, **109**, 233; (*e*) Part 5, R. Boese, G. Hägele, W. Kückelhaus, and G. Tossing, *Phosphorus Sulfur,* 1985, **25**, 103.

2 A. Baran Shortt, L. J. Durham, and H. S. Mosher, *J. Org. Chem.,* 1982, **46**, 3125; D. Valentine, jun., K. K. Johnson, W. Priester, R. C. Sun, K. Toth, and G. Saucy, *J. Org. Chem.,* 1980, **45**, 3698.

3 M. Tanaka and I. Ogata, *Bull. Chem. Soc. Jpn.,* 1975, **48**, 1094.

4 A. Hinke and W. Kuchen, *Phosphorus Sulfur*, 1983, **15**, 93.
5 H. W. Krause and A. Kinting, *J. Prakt. Chem.*, 1980, **332**, 485.
6 W. Kückelhaus, Diplomarbeit, Universität Düsseldorf, 1984.
7 R. S. Cahn, C. K. Ingold, and V. Prelog, *Angew. Chem.*, 1966, **78**, 413; V. Prelog and G. Helmchen, *Helv. Chim. Acta*, 1972, **55**, 2581.
8 S. Aime, R. K. Harris, E. McVicker, and M. Fild, *J. Chem. Soc., Dalton Trans.*, 1976, 2144 and refs. therein.
9 M. G. Gordon and L. D. Quin, *J. Org. Chem.*, 1976, **41**, 1690; L. D. Quin and L. B. Littlefield, *ibid.*, 1978, **43**, 3508; L. D. Quin, M. J. Gallagher, G. T. Cunkle, and D. B. Chesnut, *J. Am. Chem. Soc.*, 1980, **102**, 1336.
10 S. J. Featherman, L. D. Quin, and P. M. Grass, *Tetrahedron Lett.*, 1973, **22**, 1955; L. D. Quin and R. C. Stocks, *Phosphorus Sulfur*, 1977, **3**, 151.
11 W. Peters and G. Hägele, *Z. Naturforsch, Teil B*, 1983, **38**, 96.
12 A. Hinke, Dissertation, Universität Düsseldorf, 1981.
13 I. D. Campbell, C. M. Dobson, R. G. Ratcliffe, and J. P. Williams, *J. Magn. Reson.*, 1978, **29**, 397.
14 C. J. Creswell, Hamline University, St. Paul, Minnesota, U.S.A.
15 G. Bodenhausen, R. Freeman, and G. A. Morris, *J. Magn. Reson.*, 1976, **23**, 171.
16 G. A. Morris and R. Freeman, *J. Magn. Reson.*, 1978, **29**, 433.
17 A. Rauk, L. C. Allen, and K. Mislow, *Angew. Chem.*, 1970, **82**, 453 and refs. therein.
18 J. G. Smith and G. F. Wright, *J. Org. Chem.*, 1952, **17**, 1116.
19 W. Voskuil and J. F. Arens, *Recl. Trav. Chim. Pays-Bas*, 1963, **82**, 302; F. C. Whitmore and D. E. Badertscher, *J. Am. Chem. Soc.*, 1967, **55**, 1559.
20 G. Tossing, Dissertation, Universität Düsseldorf, 1983.

Received 7th November 1985; *Paper* 5/1962